

**EXPERIMENTAL AND NUMERICAL ANALYSIS OF
COMPRESSION IN 3D PRINTED FUNCTIONALLY
GRADED FOAM**

A PROJECT REPORT

Submitted by

CHANDRA SAI KRISHNA

KUMARESAN D

THIRUMOORTHY S

NITISH KUMAR S

Under the guidance of

Dr R Ramesh

In partial fulfillment for the award of the degree

of

BACHELOR OF ENGINEERING

in

MECHANICAL ENGINEERING



PSG INSTITUTE OF TECHNOLOGY AND APPLIED RESEARCH

COIMBATORE-641062

ANNA UNIVERSITY: CHENNAI 600025

ANNA UNIVERSITY: CHENNAI 600025

BONAFIDE CERTIFICATE

Certified that this project report “**EXPERIMENTAL AND NUMERICAL ANALYSIS OF COMPRESSION IN 3D PRINTED FUNCTIONALLY GRADED FOAMS**” is the Bonafide work of “**CHANDRA SAI KRISHNA, KUMARESAN D, THIRUMOORTHY S, NITISH KUMAR S**” who carried out the project work under my supervision

Dr N Saravanakumar

HEAD OF DEPARTMENT

Department of Mechanical
Engineering
PSG Institute Of Technology
And Applied Research
Coimbatore

Dr R Ramesh

SUPERVISOR

Professor
Department Of Mechanical
Engineering
PSG Institute Of Technology
And Applied Research
Coimbatore

INTERNAL EXAMINER

EXTERNAL EXAMINER

ACKNOWLEDGEMENT

We wish to express our sincere thanks to **Dr G CHANDRAMOHAN**, Principal, PSG Institute of Technology and Applied Research for his support in carrying out the project as a part of our curriculum.

We express our gratitude to **Dr N SARAVANAKUMAR**, Head of the Department, Department of Mechanical Engineering, PSG Institute of Technology & Applied Research for his constant encouragement throughout the project work.

We express our gratitude to **Dr R RAMESH**, Professor, Department of Mechanical Engineering who gave valuable guidance in helping to complete the project and without whom our project couldn't have been completed. Thank you for your comments on the methodologies and suggestions.

We would also like to express our gratitude to **Dr A S PRASANTH**, Assistant Professor (Sr Gr), Department of Mechanical engineering, PSG College of Technology who gave valuable guidance and assistance. Thank you for your comments and suggestions.

We would also like to express our gratitude towards the staff of **Material Testing Laboratory**, PSG ITECH for accepting our request to 3D print our prototypes and to test the prototypes.

ABSTRACT

Functionally graded materials (FGMs) are novel composite materials with the gradual variations in their compositions and structure throughout their volume and hence locally tailored properties. The FGMs can be manufactured by using metal foams, polymer foams. Polymer foams find a wide range of applications, including in pillows and mattresses, physical insulation, furniture, engineering materials, housing decoration, and electronic devices, etc. In comparison to metallic and inorganic (e.g., ceramic and glass) porous materials, polymeric porous materials are of interest as they are substantially lighter (because of their lower density), have lower cost, offer a wider range of compressive strengths (from elastic to flexible to semi-rigid to rigid), and are producible at considerably lower temperatures using a range of methods, including spray foaming.

The polymer foams were initially modelled in three different pore sizes varying across the volume. The configuration was 3D printed using a laser sintering metal additive manufacturing technique. Subsequently, quasi-static compression tests were conducted and their stress-strain curves were examined to ascertain the proof stress of the configurations. A numerical simulation of the compressive behaviors of the foam was then conducted and the results were correlated with those from experimentation to quantify the error in simulation. The compression tests revealed that the compressive strength was a function of density and porosity of the polymer foams. Further, the numerical results of compression behavior were validated, with less than 5 % deviation from the experimental results for the foam configurations.

TABLE OF CONTENTS

CONTENT	PAGE NO
ACKNOWLEDGEMENT	III
ABSTRACT	IV
LIST OF TABLES	VII
LIST OF FIGURES	VIII

CONTENT	PAGE NO
1. INTRODUCTION	1
1.1. CLASSIFICATION OF FGM	2
1.2. AREAS OF APPLICATIONS OF FGM	4
1.2.1. Aerospace	4
1.2.2. Medicine	5
1.2.3. Defense	5
1.2.4. Energy	5
1.2.5. Optoelectronics	5
1.3. CELLS	6
1.3.1. Open cell	6
1.3.1.1 Features and advantages of open cell foam	6
1.3.1.2 Applications of open cell foam	7
1.3.2 Closed cell	7
1.3.2.1 Features and advantages of closed cell foam	8
1.3.2.2 Applications of closed cell foam	8
1.4 MANUFACTURIG OF POLYMERIC FOAMS	8
1.4.1 Batch Foaming	9
1.4.2 Foam Extrusion	10
1.4.3 Foam Injection Molding	11
1.4.4 Fused Deposition Modeling	12

2.	MATERIALS AND METHODS	14
2.1.	MODELLING OF POLYMERIC FOAMS	14
2.2.	ANSYS ANALYSIS	16
2.2.1.	Workbench project schematics	16
2.2.2.	Engineering data	16
2.2.3.	Geometric modeling	17
2.2.4.	Symmetric modeling	18
2.2.5.	Mesh	18
2.2.6.	Analysis setting	19
2.2.7.	Solution	22
2.2.7.1.	GPU acceleration	23
2.2.7.2.	Virtual memory	23
3.	3D PRINTING OF PLA FOAMS	24
3.1	Functionally graded foam	24
3.2	Non-Functionally graded foam	24
4.	COMPRESSIVE TEST ON PLA FOAMS	26
4.1.	RESULTS OF COMPRESSION TEST	27
4.2.	COLLAPSE MECHANISM OF METAL FOAMS	32
4.2.1.	Homogenous collapse	32
4.2.2.	Progressive compression	33
4.2.3.	Quasi-static failure followed by densification	33
4.3.	DATA FROM THE GRAPH	36
5.	ANALYSIS OF THE RESULTS	37
6.	CONCLUSION	38
7.	REFERENCES	39

LIST OF TABLES

TABLE NUMBER	CONTENT	PAGE NUMBER
1	Specification Of Polymer Foams	14
2	Material Properties For Simulation Model	25
3	Energy Absorption	36

LIST OF FIGURES

FIGURE NUMBER	FIGURE NAME	PAGE NUMBER
1	FGM based on nature of gradient	3
2	FGM based on gradation	4
3	Batch Foaming	10
4	Foam Extrusion	10
5	Foam Injection Molding	12
6	Fused Deposition Modeling	13
7	CAD model of FGM	15
8	CAD model of Non-FGM	15
9	Material Property Table	16
10	Geometric Model 1	17
11	Geometric Model 2	17
12	Setting Reference Frame	18
13	Meshed model	19
14	Setting details	20
15	Selection of fixed support	20
16	Defining Components	21
17	Total Deformation	22
18	Virtual Memory Allocation	23
19	Simplify 3D software interface	25
20	Build statistics of 3D printing	25
21	3D Printed Foams	27
22	Compressive stress strain behaviour of FGM and Non-FGM foam	28
23	Stress Strain curve of FGM Foam	29
24	Stress Strain curve of Non-FGM Foam	29
25	FGM foam after compression test	31
26	Non-FGM foam after compression test	31

1. INTRODUCTION

Functionally graded materials (FGM) are advanced engineering materials that exhibit a gradual and controlled positional change of at least one property. This can be achieved by changing the volume fraction of constituents, microstructure of material type from one location to another. FGMs replace the sharp transition of properties with smooth and continuous varying properties of the material such as physical, chemical, and mechanical like Young's Modulus, Poisson's ratio, Shear Modulus, density, and coefficient of thermal expansion in a desired spatial direction. The gradual changes in volume fraction of constituent and non-identical structure at preferred direction give continuous graded properties like thermal conductivity, corrosion resistivity, specific heat, hardness, and stiffness ratio.

All these advantages made FGMs far better than homogenous composite material to use in multiple applications. Due to prominent characteristics of FGMs, several efforts have been put from time to time by researchers to enhance the properties of FGMs. Several types of FGMs have been introduced up till now based on size and structure. In this project we are manufacturing the FGM by 3D printing using polymer foams. Polymer foams are an important class of engineering material that are finding diverse applications, including as structural parts in automotive industry, insulation in construction, core materials for sandwich composites, and cushioning in mattresses. The vast majority of these manufactured foams are homogeneous with respect to porosity and structural properties.

In contrast, while cellular materials are also ubiquitous in nature, nature mostly fabricates heterogeneous foams, e.g., cellulosic plant stems like bamboo, or a human femur bone. Foams with such engineered porosity distribution (graded

density structure) have useful property gradients and are referred to as functionally graded foams. Functionally graded polymer foams are one of the key emerging innovations in polymer foam technology. They allow enhancement in properties such as energy absorption, more efficient use of material, and better design for specific applications, such as helmets and tissue restorative scaffolds. Here, following an overview of key processing parameters for polymer foams, we explore recent developments in processing functionally graded polymer foams and their emerging structures and properties.

Polymer foams are largely classified into open cell and closed cell foams and the manufacturing method varies based on that. Though there are many existing methods to manufacture closed cell foams there are only a limited methods through which open cell foams can be manufactured, the repeatability and the accuracy of the pore size cannot be fine-tuned in such manufacturing methodologies, hence by introducing a new additive manufacturing method the various design parameters can be easily fine-tuned without any changes to the manufacturing machinery. The applications for open cell metal foams are far and wide, they are usually widely used in heat exchange methods, filters, catalysts and energy absorption units.

1.1 CLASSIFICATION OF FGM

Functionally Graded Materials can be compositionally or micro structurally graded. They come in several types, depending on their constituents like ceramic- metal, metal- metal etc. Depending upon the nature of gradient, the functionally graded materials (composites) may be grouped into following types

- (a) Fraction gradient type
- (b) Shape gradient type
- (c) Orientation gradient type
- (d) Size (of material) gradient type

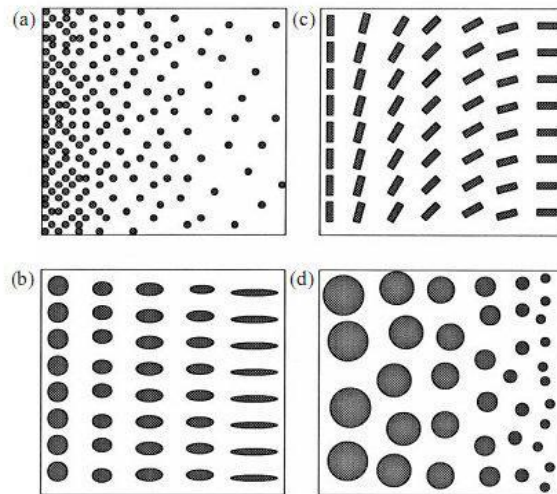
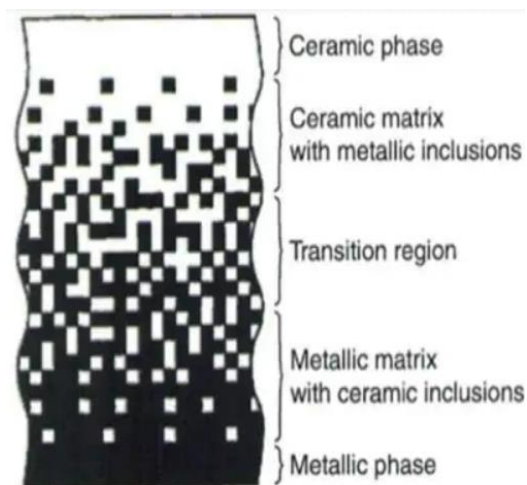


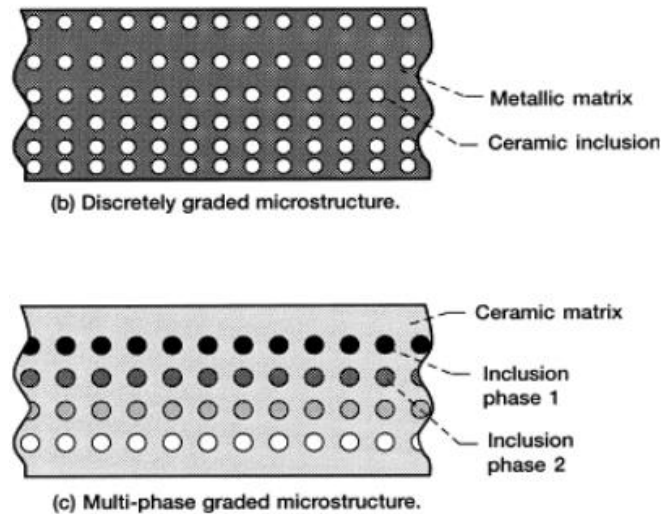
Fig 1: FGM based on nature of gradient

Based on the gradation of the Functionally Graded Material they are also further classified into the following types

- (a) Continuous
- (b) Stepped



(a)



(b)

Fig 2: FGM based on gradation

1.2 AREAS OF APPLICATIONS OF FGMS

FGMs find various applications in aerospace, automobile, medicine, sport, energy, sensors, optoelectronics etc. Owing to the importance of FGM applications, there are lots of research efforts at improving the material processing, fabrication processing and properties of the FGM. Some of the application areas of FGMS are given below

1.2.1 Aerospace

FGMs possess very high thermal gradient resistivity, which makes them suitable for thermal protection of space vehicles, for use in structures and materials for space plane body, rocket engine components and are promising in wider areas of aerospace industry. Ceramic-metal FGMS are particularly suited for thermal barriers in space vehicles. They have the added advantage that the metal side can be bolted onto the airframe rather than bonded as are the ceramic tiles used in the Orbiter. Other possible uses include combustion chamber insulation in ramjet or scramjet engines.

1.2.2 Medicine

Living tissues like bones and teeth are characterized as functionally graded material from nature, to replace these tissues, a compatible material is needed that will serve the purpose of the original bio-tissue. The ideal candidate for this application is functionally graded material. FGM has find wide range of application in dental and orthopedic applications for teeth and bone replacement.

1.2.3 Defense

One of the most important characteristics of functionally graded material is the ability to inhibit crack propagation. This property makes it useful in defense application, as a penetration resistant material used for armor plates and bullet-proof vests.

1.2.4 Energy

FGMs are used in the energy industry as energy conversion devices and as thermoelectric converters for energy conservation. They also provide thermal barriers and are used as protective coating on turbine blades in gas turbine engines.

1.2.5 Optoelectronics

FGMs are used in optoelectronics as graded refractive index materials and in audio-video discs magnetic storage media. They are now used as nano, optoelectronic and thermoelectric materials also. Other areas of application are: cutting tool insert coating, automobile engine components, nuclear reactor components, turbine blade, heat exchanger, tribology, sensors, fire retardant doors, etc. The list is endless and more applications are springing up as the processing technology, cost of production and properties of FMGs improves.

1.3 CELLS

Porous plastic foam is on the cutting edge of insulation of heat, vapour, noises and the other elements. The two major variants of porous plastics are open and closed cell foams. Both these types of foams are used in everyday products, but because of their structural difference, one type of foam may perform better than the other depending on their desired application.

1.3.1 OPEN CELL

Open cell foam is designated to vapor semi-permeable as the formation of the cells in the material is broken, rather than closed. Similar to the holes inside a sponge, air can penetrate the open cells more easily, making open cell foam more porous and absorbent than closed cell foam, which can lead to degraded performance, especially for thermal applications. Open cells are lightweight, soft and more flexible. It is easy to produce open cell foam and thus they are economical. Open cell foam can also be manufactured at both high and low densities. It is less durable than a closed cell.

1.3.1.1 FEATURES AND ADVANTAGES OF OPEN CELL FOAM

- It doesn't contain any volatile organic compounds or ozone depleting gases
- It is ideal for minimizing noise transmission
- It produces little or no residual particles, and traps most foreign particles in its pore spaces, making it ideal for reducing dust and allergens
- It is mold growth resistant

- It is good at sound proofing
- It has a good insulation value of approximately R-4.21 per inch
- It accounts for about 40-50% of heat gain/loss in apartments
- It is durable and will not break, shrink or diminish over time
- It has a high expansion capacity, capable of expanding up to 100 times
- It has a low density of between 6 and 20 kg/m³.

1.3.1.2 APPLICATION OF OPEN CELL FOAM

Open cell foam can be used for a wide range of construction purposes including:

- Low cost furniture upholstery
- Interior design projects
- Sound proofing for buildings
- Foam protective packaging
- Vapor, moisture and air permeable required application

1.3.2 CLOSED CELL

Closed cell foam is a strong, flexible plastic rubber material that's made up of internal pores or cells. These internal cells of closed cell foam sit closely together but are not connected. Closed cell structure can be compared to a net filled with bubbles, where the balloons are trapped tightly against each other, but each of the bubbles are not interconnected. The materials which can be used to produce the closed cell foam vary greatly from EVA, polyethylene, polystyrene, rubber to polypropylene etc. The closed cell foam principally contains trapped gas bubbles which are formed during the expansion and cure of the foam. These bubbles constitute a blowing agent. They are permanently locked to a place, as the trapped gas is very efficient in increasing the insulation capability of the foam. The foam which is formed is strong and is

usually of a medium density which enables the gas bubbles to lock into place. The nature of the foam enables it to be vapor retardant and resist liquid water.

1.3.2.1 FEATURES AND ADVANTAGES OF CLOSED CELL FOAM

- Helpful and extremely reliable to be used in both exterior and interior environments
- Helpful in increasing the structural strength
- Best for providing heat and sound insulation
- Effectively reduce the vapor transmission
- Superior moisture barrier
- Excellent resistance to leakage

1.3.2.2 APPLICATIONS OF CLOSED CELL FOAM

- Insulation and sealing for construction and building
- The appliances and HVAC system
- Thermal insulation and shock absorption
- The seals of enclosure and cabinets
- The medical disposables
- The equipment of gas and oil
- Aerospace and aircraft
- The transportation and automotive

1.4 MANUFACTURING OF POLYMERIC FOAMS

The principle of foaming processes includes the steps of polymer saturation or impregnation with a foaming agent, providing super saturated polymer-gas mixture by either sudden increment of temperature or decrease in pressure, cell

growth, and stabilization. In thermoplastic foaming processes, it is important to obtain foams with closed cell structure with thin polymer cell walls covering each cell. In order to provide this structure, cell growth must be controlled through the process. Temperature limit is critical in obtaining microcellular structure. If temperature is higher, then melt strength of the polymer can be low-inducing cell rupture. On the other hand, if temperature is too low, this will result in longer foaming times and increment in viscosity of the polymer. As a consequence, cell growth will be restrained, and insufficiently foamed products will be obtained. Therefore, the process conditions have serious importance on cell morphology of the polymer foams. The most known thermoplastic foaming processes are batch foaming, extrusion foaming, and foam-injection molding.

1.4.1 BATCH FOAMING

Batch foaming can be applied in two different methods as follows, pressure-induced method and temperature-induced method. In pressure-induced method, polymer is saturated with blowing agent in an autoclave, and then, cell nucleation is done by sudden depressurization of the system to atmospheric pressure. The final cell morphology is obtained by either cooling the polymer in a solvent or by cooling it within air. In temperature-induced batch foaming, the beginning of the process is similar to pressure-induced foaming but at lower temperatures. After saturation is completed, the sample is taken out of the autoclave and put into hot oil bath between the temperatures of 80–150°C for a period of time in order to obtain cell generation. After this step, the sample is put into a cooling bath of water or a solvent as shown in Fig3. The important point in batch foaming is the geometry of the plastic samples. They are generally a circular disc, rectangular, or square shape with the thickness between 0.5–3 mm not to hinder gas diffusivity.

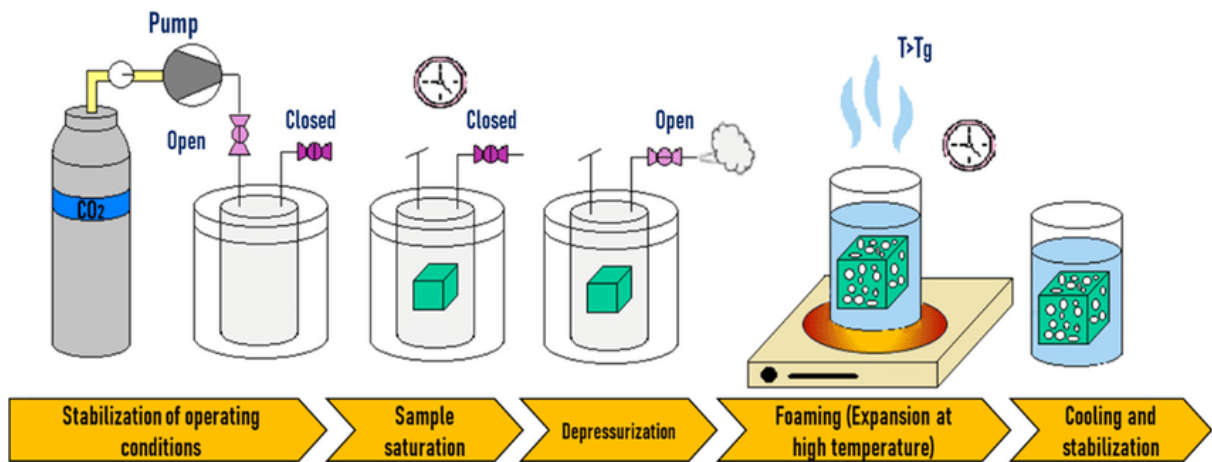


Fig3: Batch foaming

1.4.2 FOAM EXTRUSION

In foam extrusion, a tandem line extrusion machine is equipped with a gas supply as shown in Fig4. Typical product types are thermoplastic-based foamed sheets, pipes, and expanded tubes. The pellets supplied from the hopper into the barrel are melted under high pressure and blowing agent. CO₂ gas in supercritical condition is injected into the polymer. Due to the high pressure in the barrel, nucleation of the foam cells is prevented.

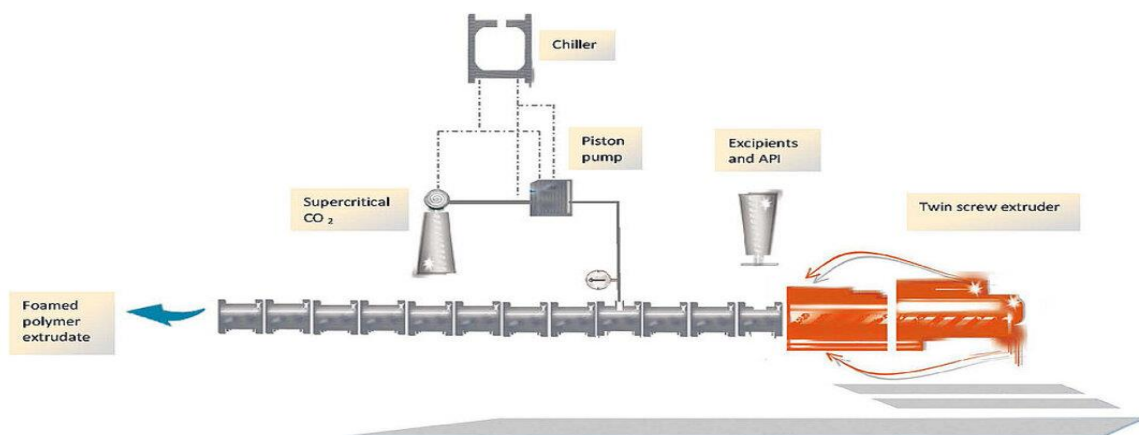


Fig4: Foam Extrusion

As the polymer exits from the die, foam cells are generated by the sudden pressure drop. The final step is cooling, calibration, and cutting of the extruded foams. The extrusion foaming process can be either physical or chemical foaming. physical foaming is shown that a gas supply is integrated to the extruder. In industrial applications, chemical foam extrusion is also applied due to its cheapness in tooling. In chemical foam extrusion, polymer pellets and chemical foaming agent are mixed through the barrel, and the heat in the barrel decomposes the chemical foaming agent resulting in gas which provides expansion of the polymers as it exits the die.

Melt temperature is critical in decomposition of the foaming agent. The pressure must be high enough in order to keep the dissolved gas in the polymer before it exits the die. If the pressure and temperature are not set correctly, foaming agent will not be decomposed and can induce left particles or agglomerations of foaming agent, which can lead to poor cell morphology and poor surface quality.

The most known chemical foaming agent is azodicarbonamide (ADC), an exothermic chemical foaming agent. It releases high-amount of N₂ gas together with CO₂ in lower amount into the polymer. However, due to the toxic by-products of ACD, endothermic type commercial foaming agents are being used, such as Clariant's Hydrocerol.

1.4.3 FOAM INJECTION MOLDING

Foam injection molding is similar to conventional injection molding, but an additional gas unit is integrated to the injection molding machine if physical foaming is applied. There are currently three widely known foam injection–

molding technologies available to produce microcellular foams using CO₂ as a physical blowing agent.

Foam injection molding has some critical points to be considered. One of them is the presence of the back pressure. If back pressure is not applied, polymer-gas mixture would move the screw axially and instability in dosing of the polymer would be seen. Also, foaming agent would expand in the plasticization unit and leak out during injection. This would prevent cell generation in the polymer. The second critical point in foam injection molding is the selection of needle shut off nozzle that prevents the leak out of the nozzle and gas loss.

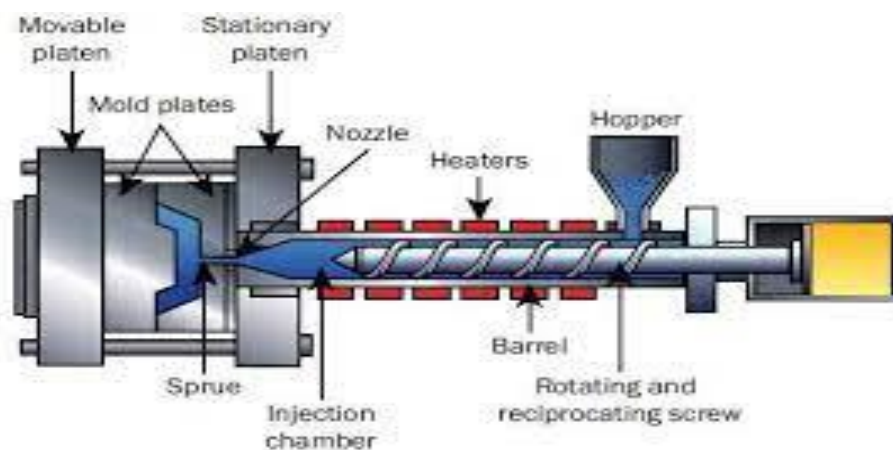


Fig5: Foam Injection Molding

1.4.4 FUSED DEPOSITION MODELING (FDM)

The Fused Deposition Modeling (FDM) process constructs three-dimensional objects directly from 3D CAD data. A temperature-controlled head extrudes thermoplastic material layer by layer.

The FDM process starts with importing an STL file of a model into a pre-processing software. This model is oriented and mathematically sliced into

horizontal layers. A support structure is created where needed, based on the parts position and geometry. After reviewing the path data and generating the toolpaths, the data is downloaded to the FDM machine.

The system operates in X, Y and Z axes, drawing the model one layer at a time. This process is similar to how a hot glue gun extrudes melted beads of glue. The temperature-controlled extrusion head is fed with thermoplastic modelling material that is heated to a semi-liquid state. The head extrudes and directs the material with precision in ultrathin layers onto a fixtureless base. The result of the solidified material laminating to the preceding layer is a plastic 3D model built up one strand at a time. Once the part is completed the support columns are removed and the surface is finished.

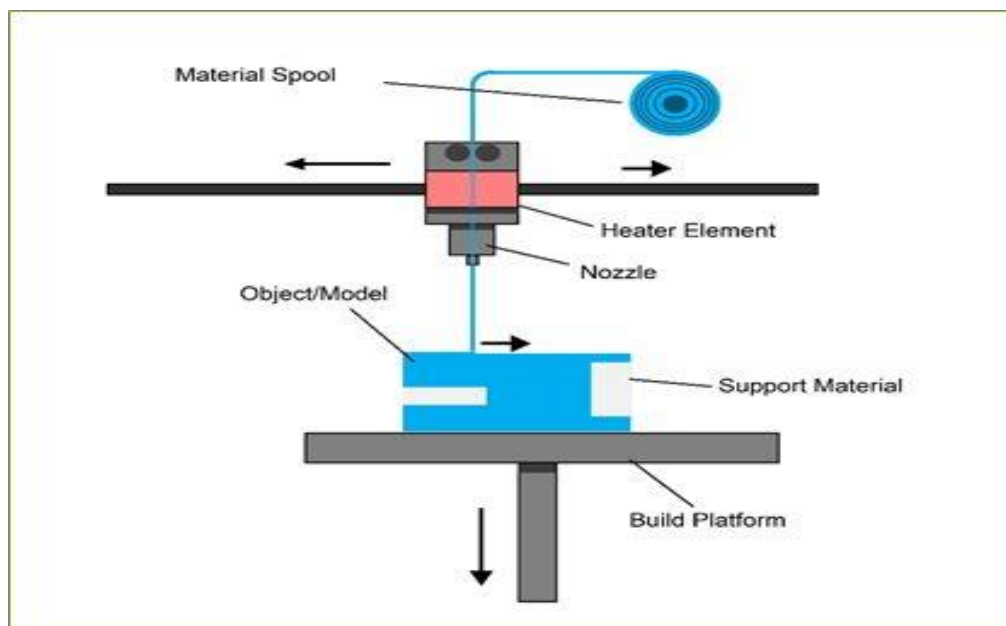


Fig6: Fused Deposition Modeling

2. MATERIALS AND METHODS

The steps followed in modelling, 3D printing, compression testing and simulation are delineated in this section, here under.

2.1 MODELING OF POLYMERIC FOAMS

The open cell polymeric foams were initially modelled using Solid works designing software. Two open cell foams of dimensions 1 inch cube (25.4 x 25.4 x 25.4mm³) were modeled. One of the specimens consisted of three pore sizes of 3mm, 2.5 mm and 2 mm and the other specimen consisted of 2.5 mm throughout its height as listed in table 1. The strut thickness of the foams varied in the range of 0.7mm to 1 mm to ensure structural stability and to avoid premature collapse of the foam during 3D printing

$$p = \frac{\rho_w - \rho_f}{\rho_w} \times 100 \quad (1)$$

The porosities of the foams were determined using equation (1) where, ρ_w is the density of foam structure without pores and ρ_f represents the density of the porous foam. The specimen densities are listed in table 1.

Table 1 Specifications of metallic foams.

Sl.N o	Designation	Height (mm)	Pore Size (mm)	Porosity (%)	Density (kg/m ³)
1.	Specimen 1	25	2.0	15.1	1052.76
		25	2.5		
		25	3.0		
2.	Specimen 2	75	2.5	17.99	1016.83

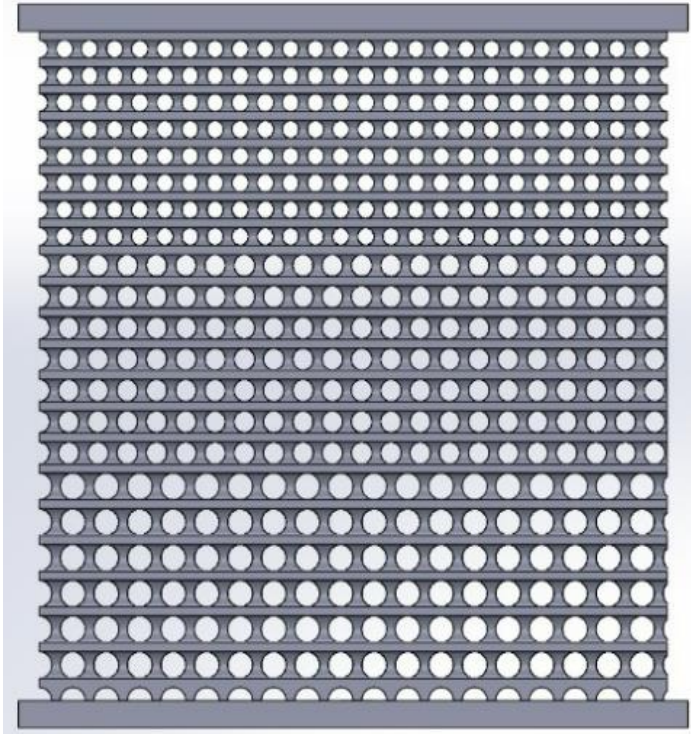


Fig 7: CAD model of FGM

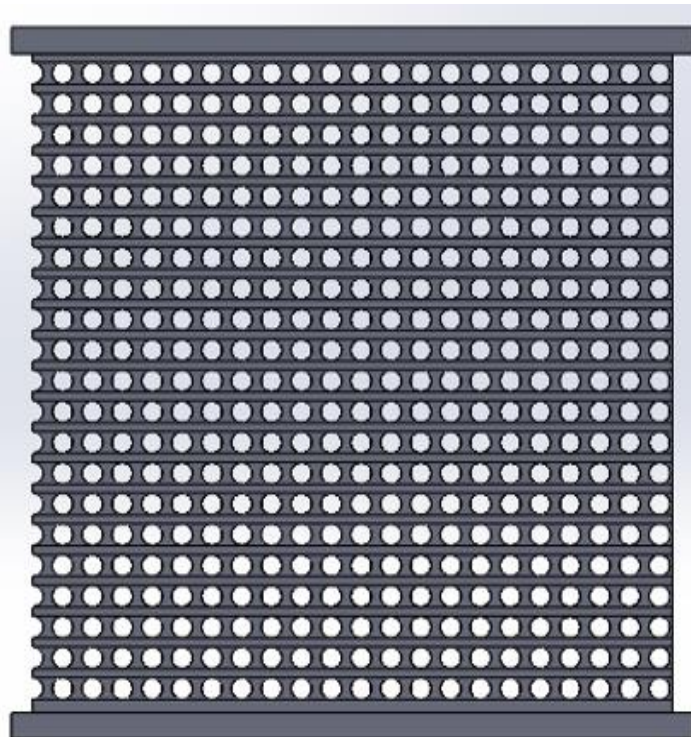


Fig 8: CAD Models of Non-FGM

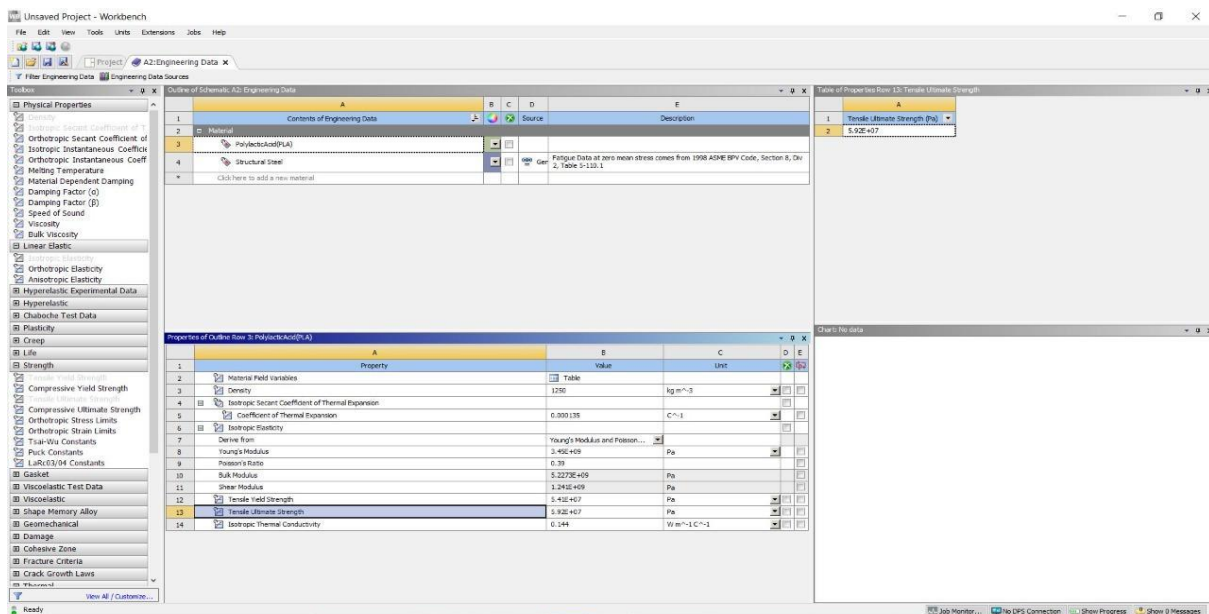
2.2 ANSYS ANALYSIS

2.2.1 WORKBENCH PROJECT SCHEMATICS

The module used for this type of test is Transient Structural as the force varies with time in this type of analysis.

2.2.2 ENGINEERING DATA

The material used for the metal printing is PLA (polylactic acid). Therefore, the material properties of the PLA have to be uploaded to the workbench console. The material properties are obtained from the existing library of Ansys provided by GRANTA material data for simulation.



The screenshot displays the ANSYS Workbench Engineering Data interface. The central pane shows a table of material properties for Polylactide(PLA). The right-hand pane shows a table of Tensile Ultimate Strength data.

Property	Value	Unit
Material		
Polylactide(PLA)		
Structural Steel		
Click here to add a new material		

Property	Value	Unit
Material Field Variables	Table	
Density	1250	kg m ⁻³
Isotropic Secant Coefficient of Thermal Expansion		
Coefficient of Thermal Expansion	6.000135	C ⁻¹
Derive from	Young's Modulus and Poisson's Ratio	
Young's Modulus	3.45E+09	Pa
Poisson's Ratio	0.39	
Bulk Modulus	5.222E+09	Pa
Shear Modulus	3.241E+09	Pa
Tensile Yield Strength	3.42E+07	Pa
Tensile Ultimate Strength	3.92E+07	Pa
Isotropic Thermal Conductivity	0.144	W m ⁻¹ C ⁻¹

Table of Properties Row: 13: Tensile Ultimate Strength	Value
1 Tensile Ultimate Strength (Pa)	
2	5.92E+07

Fig 9: Material Property Table

As the material used is subjected to plastic deformation the data should be of non-linear nature. The non-linear data used for this specific problem is Multilinear isotropic hardening data.

2.2.3 GEOMETRIC MODELING

The geometry modeled in solid works is converted to Parasolid file and it is then imported to SpaceClaim. The body is then split by considering the symmetric regions in order to reduce the number of elements and effectively reducing the number of elements present in the model. The model is then saved as a SpaceClaim file.

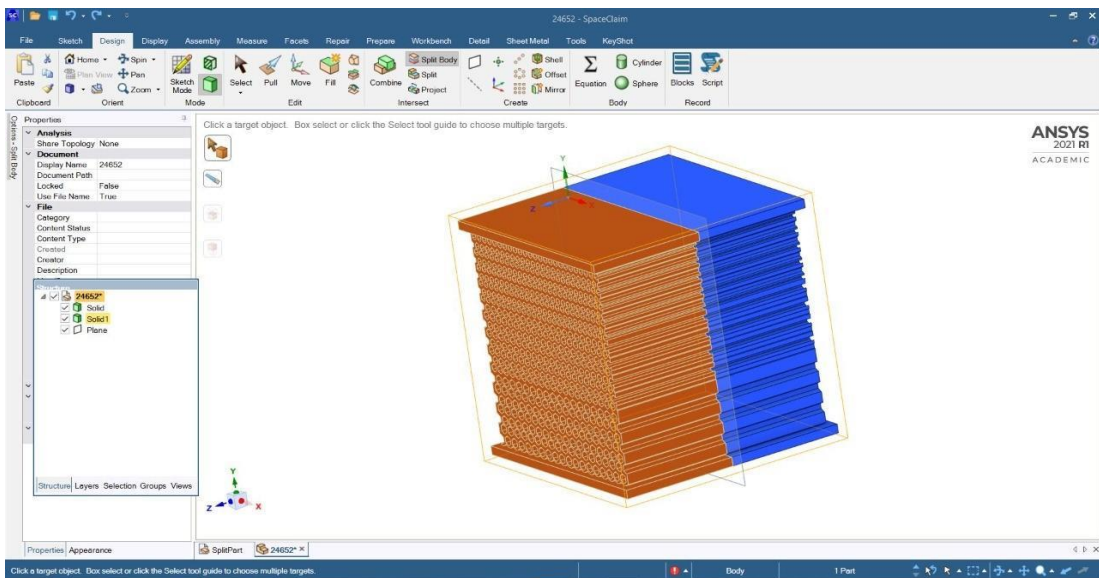


Fig 10: Geometric Model 1

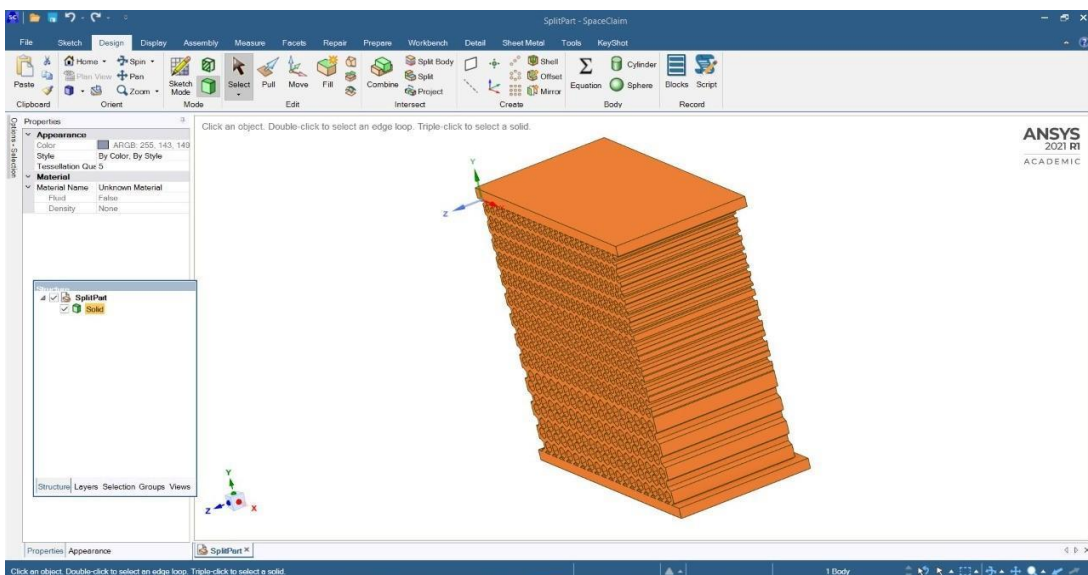


Fig 11: Geometric Model 2

2.2.4 SYMMETRIC MODELING

The Ansys is first notified of the presence of symmetry in the imported geometry. The geometry in this case is symmetric to the z axis and x axis. For this purpose of defining a new symmetric region a new coordinate system is set as a reference frame only for a symmetric region as shown in the below image.

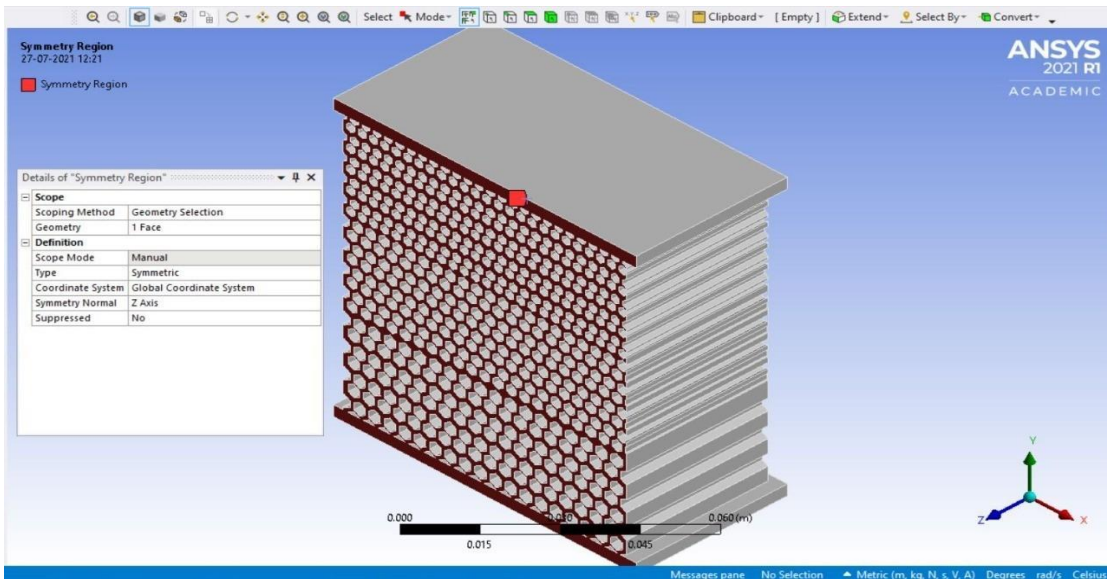


Fig 12: Setting Reference Frame

2.2.5 MESH

The mesh element is program controlled and the physical preference for the same is set to Non-linear mechanical. The maximum edge size of the mesh element is set to **1 mm** for higher accuracy. The other settings are left default.

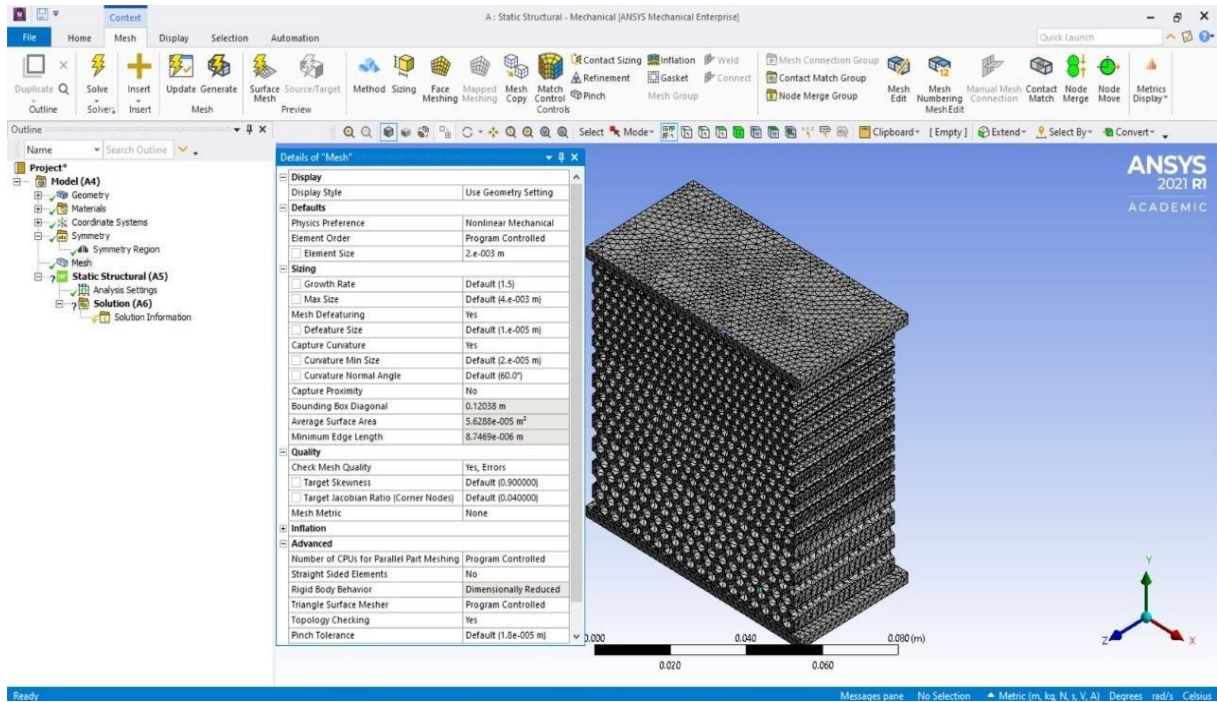


Fig 13: Meshed Model

2.2.6 ANALYSIS SETTING

In order to replicate the compression test the top surface is pushed at a velocity of 1 mm/min similar to the feed rate of the compression test machine. The step end time is set according to the maximum displacement experienced by the specimen in the compression test experiment.

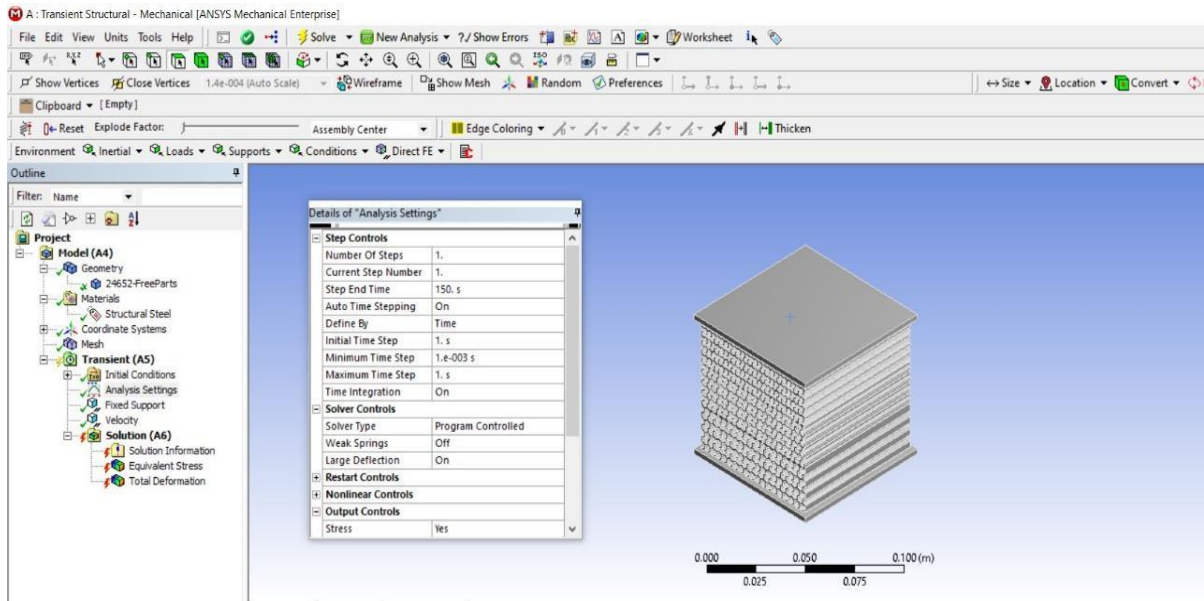


Fig 14: Setting details

1. The auto time stepping is turned on and the initial time step is set as 1 s, the minimum time step and maximum time step is set as 0.001s and 1 s respectively. This is because we need at least 100 different snapshots of the analysis

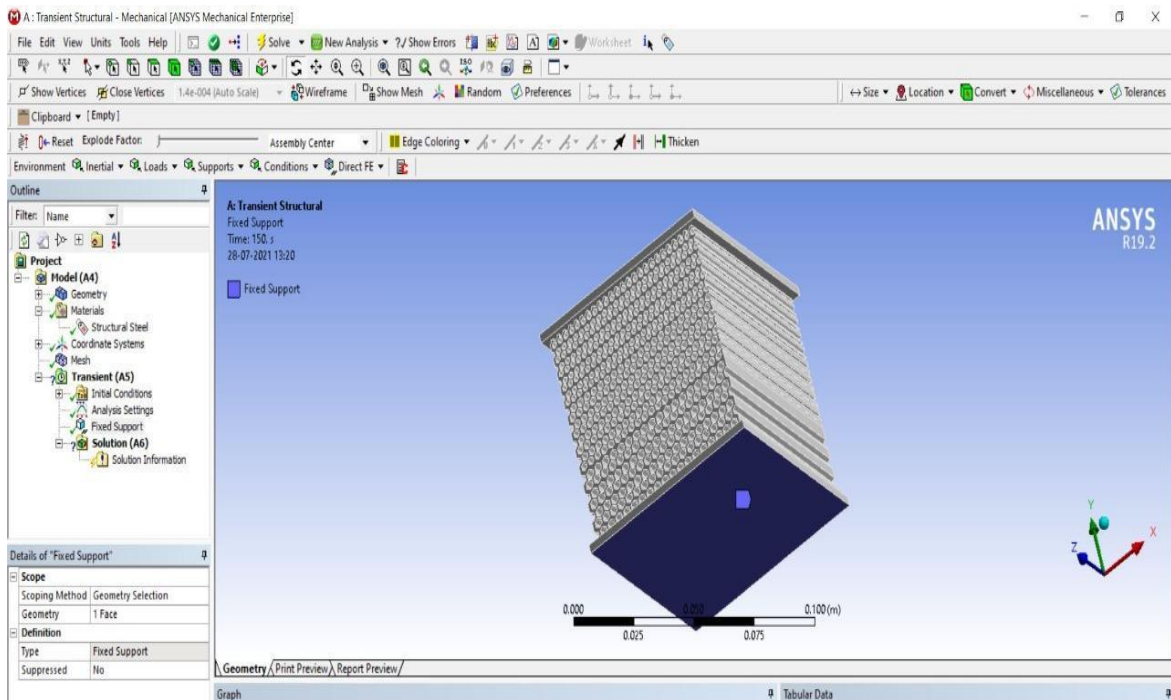


Fig 15: Selection of fixed support

2. The specimen is fixed at one end and the velocity is applied at the other end in the negative Y-Axis. All the other settings are set as default. The velocity is given as 1mm/min according to the ASTM D695 standards.

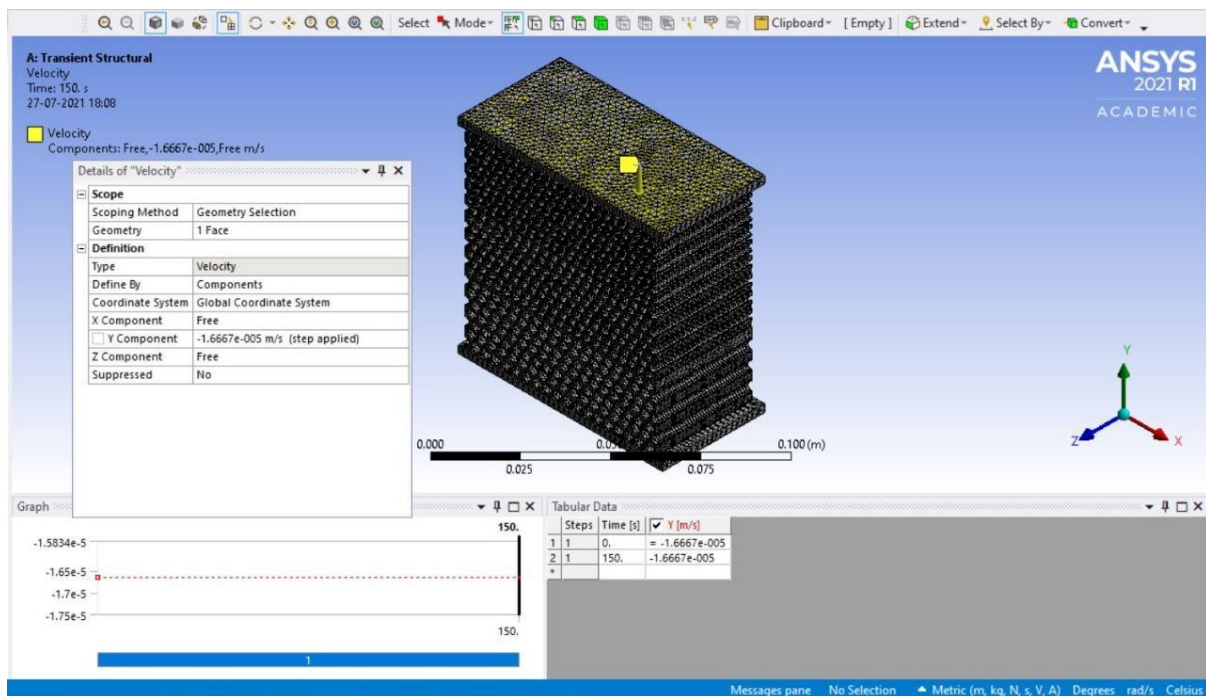


Fig 16: Defining components

2.2.7 SOLUTION

The solutions that are selected are a deformation probe and the force probe. The force probe gives the force experienced by the fixed support.

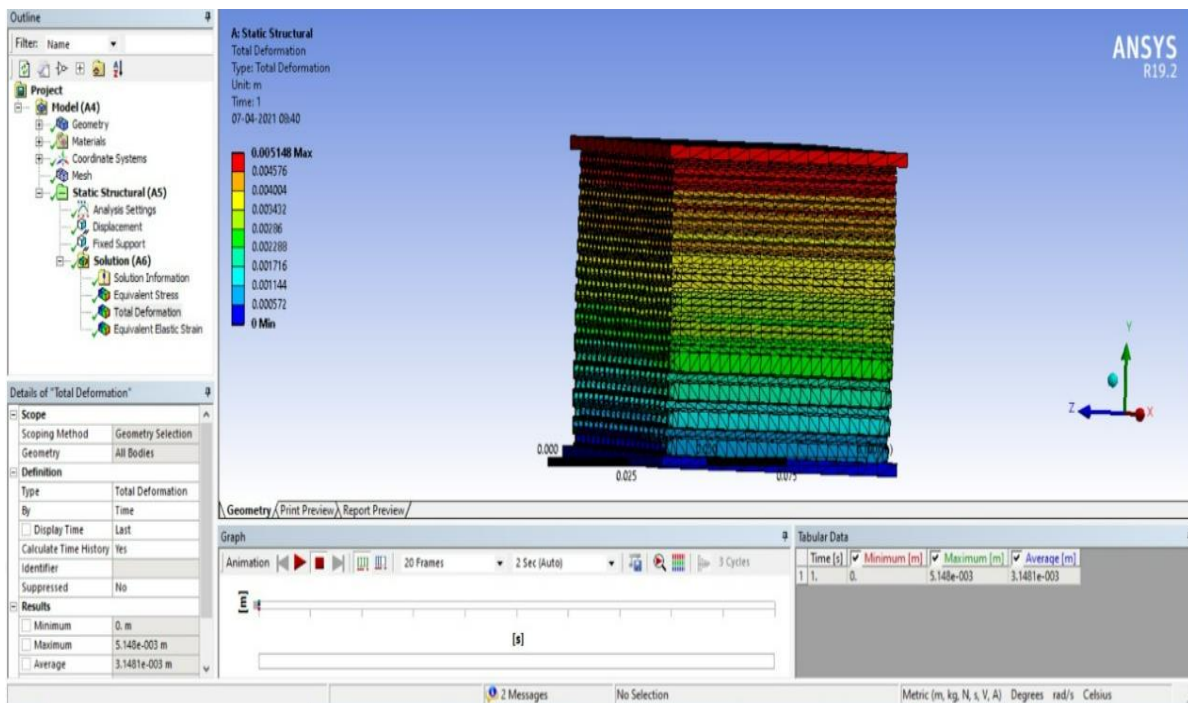


Fig 17: Total deformation

2.2.7.1 GPU ACCELERATION

In order to boost the performance gpu override command has been given and the gpu used for this analysis is **NVIDIA GeForce GTX 1650** Graphics. The GPU utilizes a Pascal architecture with a clock speed of 1665 MHz, memory speed of 8 Gbps and a frame buffer of 4 GB GDDR6. Additionally, since the GPU comprises 896 CUDA cores, it is best suited for mathematical calculations or solving complex mathematical models.

2.2.7.2 VIRTUAL MEMORY

In order to cope up with the memory requirement the virtual ram of the system was hiked up and the system managed to accommodate more memory for the problem solving.

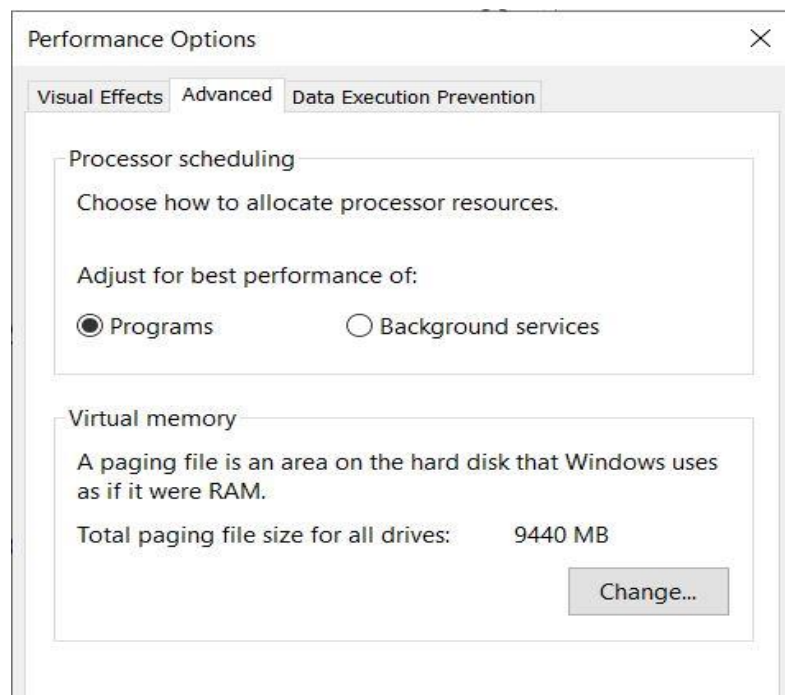


Fig 18: Virtual memory allocation

3. 3D PRINTING OF PLA FOAMS

Subsequent to modelling, the CAD models were converted to stereolithography (STL) format. The STL files were then imported to Virtual Frontier Robotics 3D printer. The three dimensionally identical specimens with varied pore sizes were 3D printed by Fused Deposition Modelling (FDM) of Polylactic acid (PLA). The 3D printing slicing software used is Simplify 3D which controls every aspect of our 3D print. It translates 3D models into instructions which the printer understands, better instructions means better print quality of our product. The bed surface type used is Aluminium with a gap of 0.001mm between bed and nozzle, the nozzle diameter and temperature are 0.4 mm and 210°C respectively. The layer height is given as 0.2mm with Infill Percentage of 70%.

3.1 3D Printing of Functionally Graded Material

The Functionally graded specimen with pore sizes 2mm, 2.5mm, 3mm varying along the height is printed with a build time of 20hrs 25minutes. The total filament length consumed is 80432.8mm with a weight of 241.83g.

3.2 3D Printing of Non-Functionally Graded Material

The Non-Functionally Graded specimen with pore size of 2.5mm along the height is printed with a build time of 19hrs and 36minutes. The total filament length consumed is 77430.5mm with a weight of 232.8g.

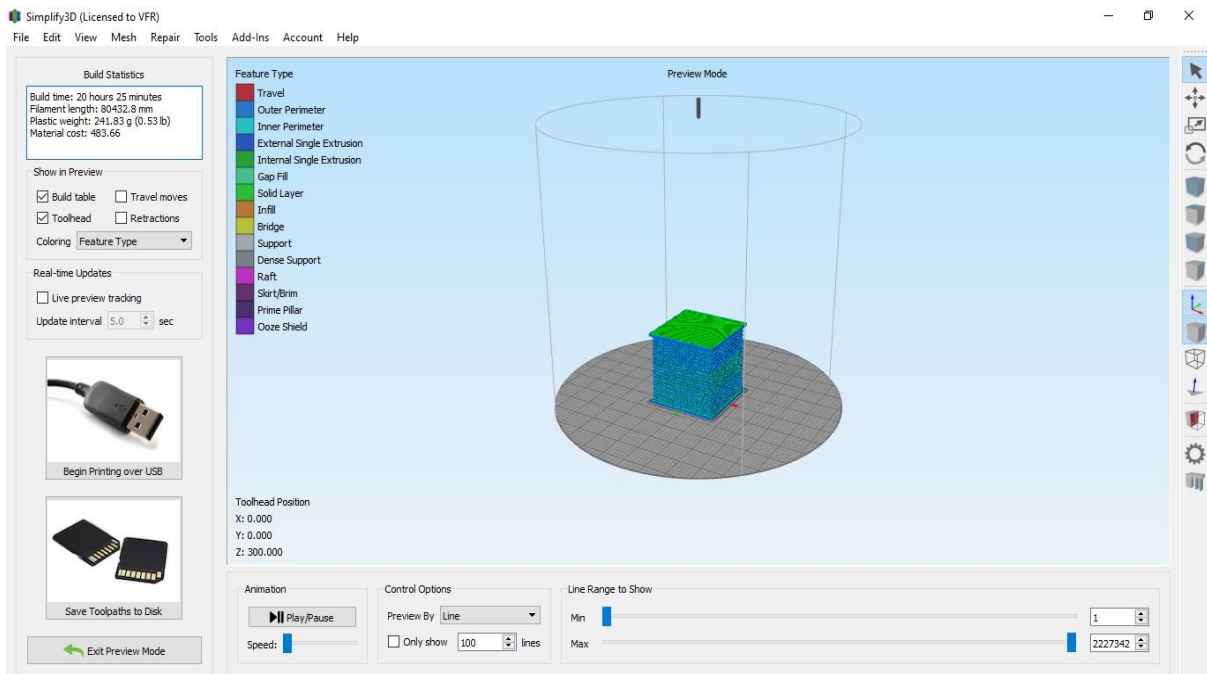
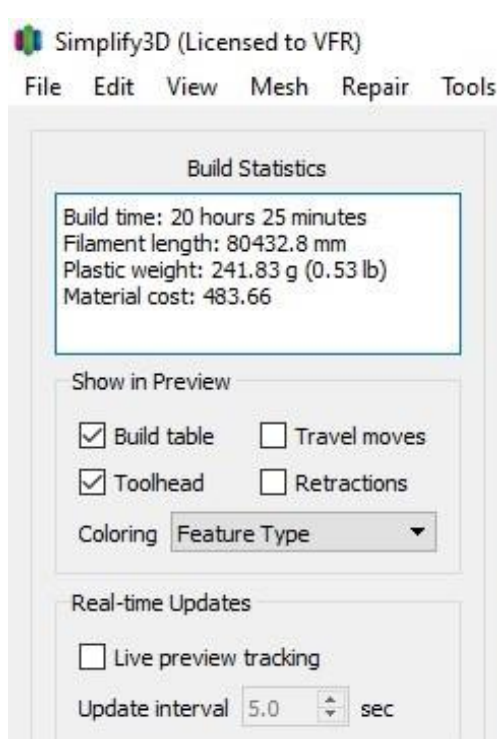
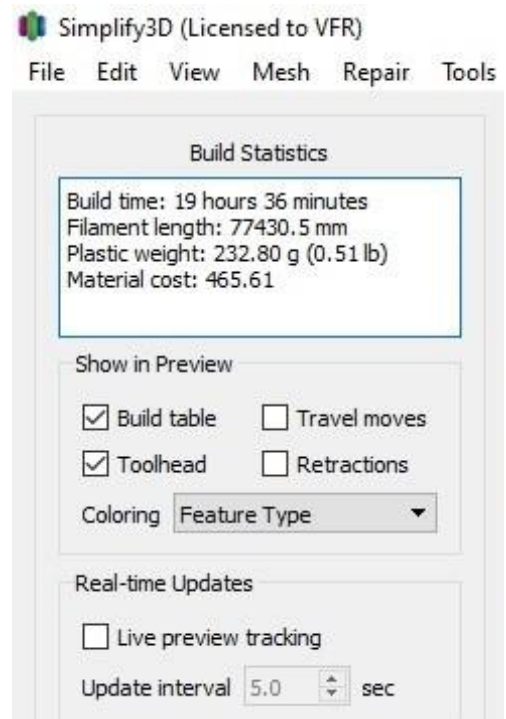


Fig 19: Simplify 3D software interface



For FGM



For Non FGM

Fig 20: Build statistics of 3D printing

4. COMPRESSIVE TEST ON PLA FOAMS

The compressive behaviour of the two specimens was assessed using the TESTRON Testing Machine with a maximum rated load capacity of 100 kN. The uniaxial compression tests for the three specimens were performed up to a strain rate of 20 % in accordance with ASTM D695 standard and with a crosshead speed of 1mm/min.

Table 2 Material Properties for simulation model.

Sl.No	Property	Value	Unit
1	Density	1240	Kg/m ³
2	Young's Modulus	3.45*10 ⁹	Pa
3	Poisson's ratio	0.39	-
4	Bulk Modulus	5.2273*10 ⁷	Pa
5	Thermal Conductivity	0.144	W/(m-K)
6	Specific Heat	1190	J/(kg-K)
7	Isotropic Ultimate Strength	5.92*10 ⁷	Pa
8	Yield Strength	5.41*10 ⁷	Pa

4.1 RESULTS OF COMPRESSION TEST

The two open cell foams were modelled using SOLIDWORKS software and then 3D printed. Below figure shows the two PLA foams ONE with three varying pore sizes of 3 mm, 2.5 mm and 2 mm and the other one with 2.5mm throughout its height. The two foams were then subjected to compressive loading.

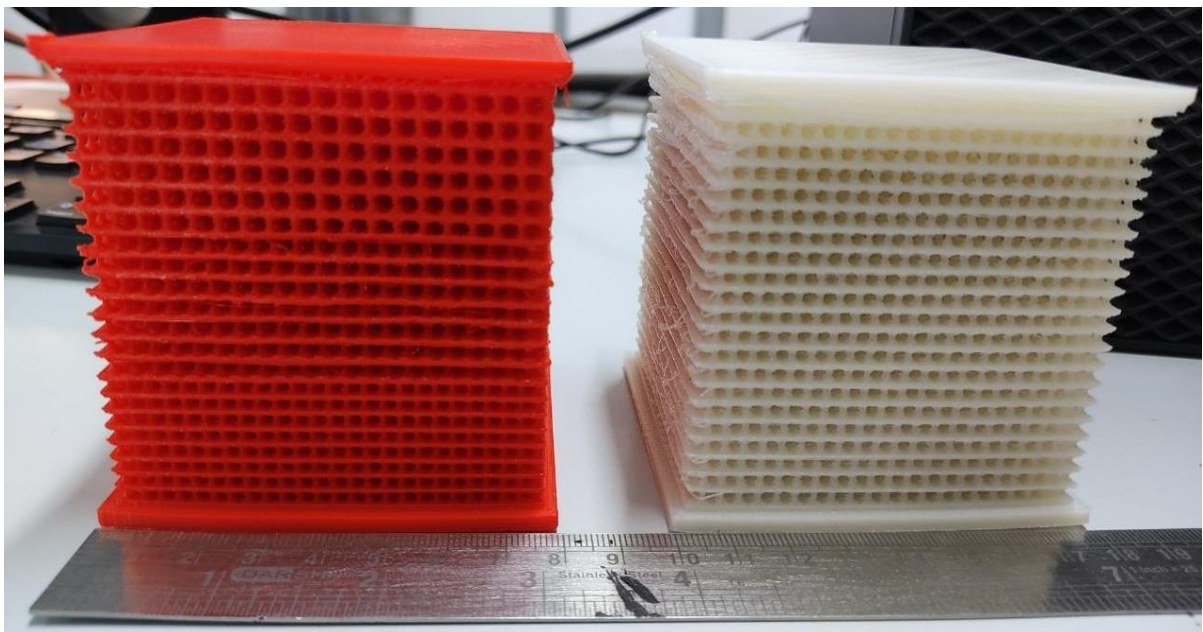


Fig 21: 3D Printed Foams

The resulting stress-strain curves of the open cell foams are plotted in the figure. The obtained stress-strain curves consist mainly of three zones, the linear elastic part, the plateau part and the densification part. When subjected to a compressive load, at first the stress was noticed to increase linearly with the applied force, thus presenting an elastic response. In the second part, it was found that the stress oscillated between the average values due to the failure of specimen cells. However, large fluctuations of the stress-strain curves can be

observed in the plateau stage for specimen1, while specimen 2 has relatively stable performance in this stage.

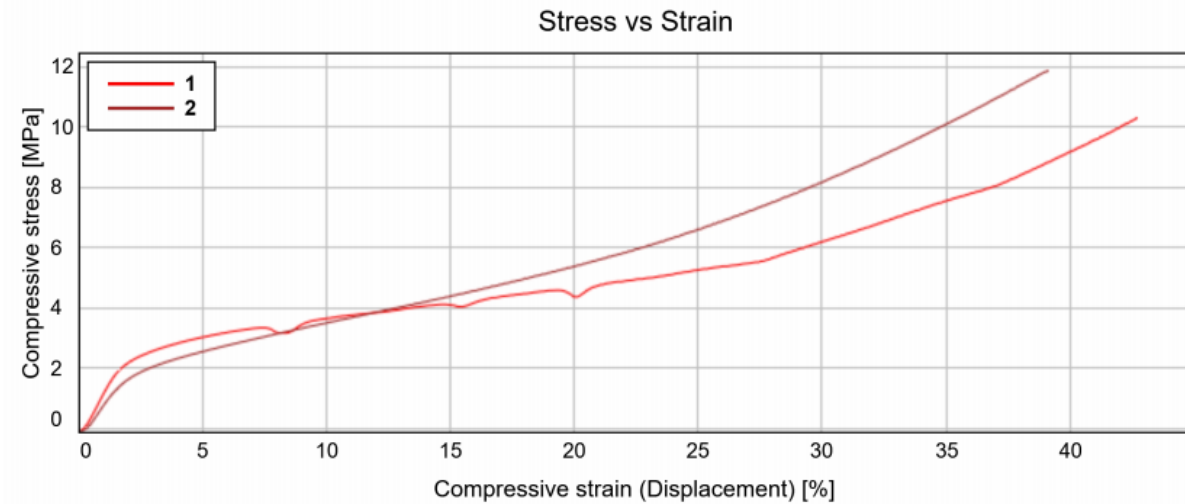


Fig 22: Compressive stress-strain behaviour of FGM and non- FGM foam

The strong fluctuation in the plateau stage of specimen 1 is related to the plastic collapse of the cell walls. The third part is characterized by a considerable increase in stress due to the densification of the cells. After analyzing the stress-strain curves, it was found that the plateau portion is not stable. There is a strain variation due to the fragile failure of the unit cell walls in the manufactured specimen, the cell walls of the layer-by-layer printed specimens contain micro-pores as printing defects. These micro-pores acted as sources of crack initiation due to the stress concentration under the action of compressive load

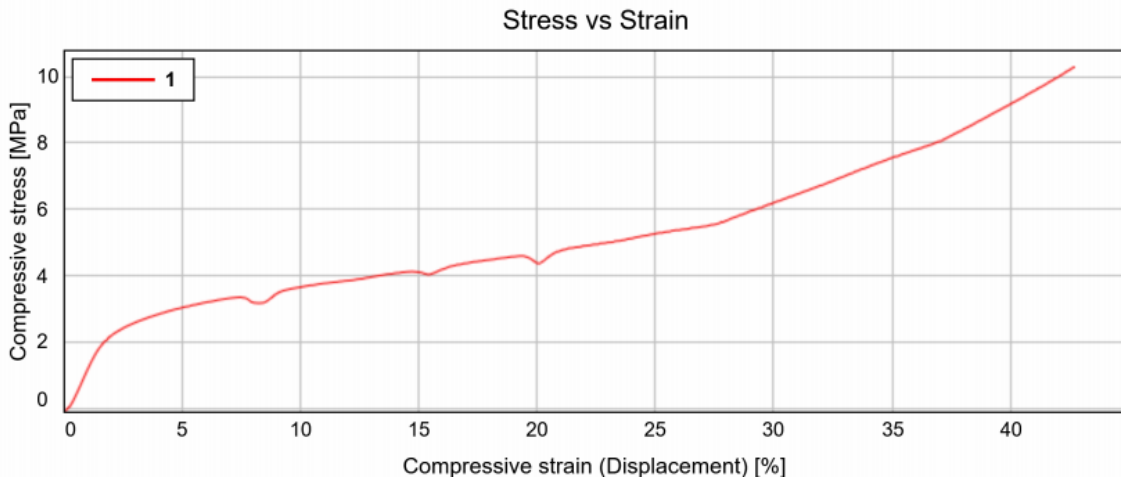


Fig 23: Stress Strain curve of FGM Foam

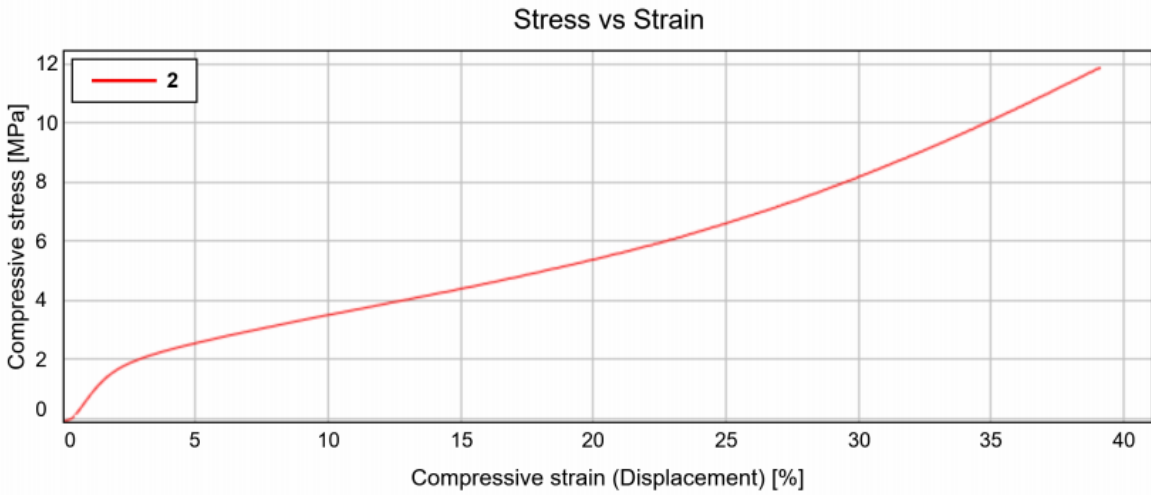


Fig 24: Stress Strain curve of Non-FGM Foam

Densification follows a two-step approach. In step 1, the failed vertical struts slip into the adjacent pores. As the applied load is further increased, these vertical struts begin to buckle, deform and ultimately fill the pore. In step 2, the deformation of vertical struts together with the applied load, initiate deformation in the form of elongation or shortening of the horizontal struts in the foam structure. The aforementioned two steps of densification occur simultaneously and randomly, throughout the specimen. The process of densification continues until all the pores have been filled by the deformed struts. At the end of densification, the specimen essentially becomes a solid. Clearly, the densification phase constitutes the largest percentage of the total deformation of the metallic foam.

In order to estimate the experimental results by computation, numerical models of the two specimens were analyzed. The top surface of each specimen was subjected to compaction at incremental velocities of 1 mm/min, identical to the feed rate of the compression test. The built-in deformation and force probes in ANSYS Workbench were utilized to estimate the deformation and force experienced by the fixed support. These values were then compared with the experimental results and the numerical error was estimated. This procedure was replicated for two specimens and it was observed that the numerical simulation was validated by experimental results with the estimated error being less than 5 %.



Fig 25: FGM Foam After Compression Test

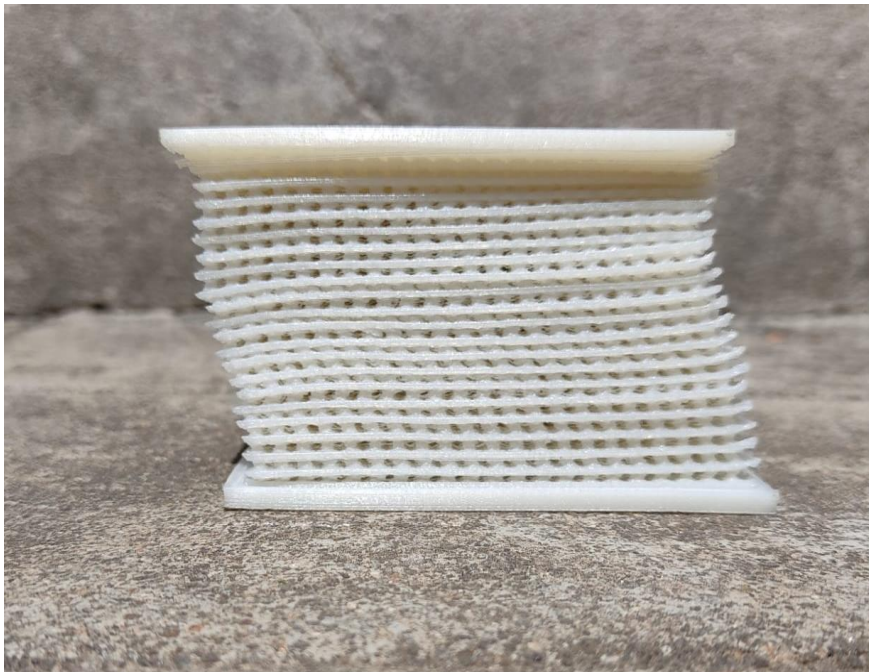


Fig 26: Non FGM Foam After Compression Test

4.2 COLLAPSE MECHANISM OF PLA FOAMS

This study primarily deals with the energy absorption properties of metal foams. It is clear that the extraordinary energy absorption characteristics of metal foams are due to the unique way of collapse of the metal foams, with larger capacity for deformation. It would greatly help the study to analyze how metal foams collapse so as to understand how energy absorption happens. The collapse of metal foams under load can occur through three different mechanisms:

1. Homogenous collapse
2. Progressive compression
3. Quasi static failure followed by densification

4.2.1 HOMOGENEOUS COLLAPSE

Homogeneous collapse is the most ideal of the three mechanisms, and assumes uniform strength throughout the material. The prerequisite is that all the struts between the pores are of exactly equal area and therefore have exactly equal load bearing capacities. If that is the case prevalent across all the layers, it then follows that under load, all the points across the specimen will deform uniformly. Therefore during homogeneous collapse, all the layers deform equally simultaneously, such that the strain in the first layer is equal to the strain in the last layer and every layer in between. Homogeneous collapse represents itself as a straight line in a graph because the stress uniformly increases with the deformation. This can only occur if every layer is perfect and there is no specific stress concentration or local failure, therefore it is a very rare phenomenon.

4.2.2 PROGRESSIVE COMPRESSION

Progressive compression is another closely approximate collapse mechanism that occurs in some cases of traditionally manufactured non uniform foams. During progressive compression, the first layer completely deforms first, without any damage to any other layers. After the complete deformation and densification of the first layer, the second layer begins to deform, and so on. Each layer is deformed separately and distinctly, after the previous layers are completely densified. This draws a very significant conclusion that during progressive compression the deformation characteristics of each layer is identical. This collapse mechanism is assumed in extremely simplified calculations regarding PLA foams, because it is sufficient to consider just one layer for any foam with any number of layers. This mechanism is seen as alternating peaks and valleys in a graph.

4.2.2 QUASI-STATIC FAILURE FOLLOWED BY DENSIFICATION

The above described collapse mechanisms occur in highly controlled ideal situations and are summed for ease of calculations. The mechanism of collapse that is very closely approximated to the observed collapse is the process of quasi-static failure followed by densification. This process takes into account the phenomena of stress concentration and local failure and is therefore more accurate and reliable. The first process of quasi-static failure is the direct effect of local failure due to stress concentration. When the foam is subjected to a compressive load, the stress is concentrated in the weakest strut in the weakest

layer. Therefore that particular weakest strut fails first, leading to the failure of all the struts in that layer consecutively. Then the next weakest strut in a weak layer fails and so on, until all the strut in all the layers have failed locally.

It can be questioned how this is different from the progressive compression mechanism of collapse but it has to be noted that while in the process of progressive compression each layer deforms and densifies completely before the next one starts to deform, in the case of quasi-static failure even at the end of local failure of all the struts, the pores are retained with a mere failure in the struts, and the density of the specimen remains largely the same, i.e., there is no densification happening during the quasi-static failure. This leads to a flat curve with alternating peaks and valleys, due to the intermittent failure of the struts. The process of densification begins after all the struts have failed locally. Densification propagates through two methods:

1. Elongation and compression of horizontal struts
2. Slip followed by buckling of vertical struts

First, the vertical struts that have failed locally slip into nearby pores. As more load is applied, these vertical struts begin to buckle, deform and ultimately fill the pore. As the vertical strut buckles and deforms, the horizontal struts begin to elongate or shorten to accommodate the buckling. It has to be taken into consideration that as a vertical strut slips into a pore and deforms, the bottom horizontal strut, i.e., the one constituting the said pore itself, begins to deform also. This results in the complete densification of the material.

These two methods of densification occur randomly and simultaneously throughout the specimen. The densification continues until all the pores have been so filled by deformed struts of the layer, and pores themselves have also deformed to accommodate it, and upon the end of densification the specimen essentially becomes solid.

Clearly, the densification phase constitutes the largest share of the total deformation and therefore most of the energy absorption happens in the densification phase. The graph of such a collapse has a flat quasi-static region and a steadily rising densification. Even though it has been mentioned that the quasi-static region has alternating peaks and valleys, compared to the large deformation and steady rise in the stress during densification phase, the peaks and valleys of the quasi-static phase are negligibly small and the curve appears flat. From the presented graphs of the results of the test specimens, it can be evidently seen that the collapse mechanism seen the third type: quasi-static failure and densification

4.3 DATA FROM THE GRAPH

Two graphs from the test specimens exhibit largely similar structures. The graphs have three regions:

- The linear elastic region
- The plateau region
- The densification region.

The linear elastic region that represents the reversible elastic bending of the struts, the stress was noticed to increase linearly with the applied force, thus presenting an elastic response. In specimen 1 this region lasts till about a strain of 1.94% and in specimen 2 this region lasts till about a strain of 1.71%, there is not much difference in the elastic region of both specimens.

The quasi-static region is the flat of the curve, and it can be seen that in the specimen1 it lasts till about a strain of 0.281. Strain is the ratio of the deformation and original height of the specimen, therefore a strain of 0.281 means the deformation is equal to the 28.1% of the height of the specimen. And from the tabular data it can be seen that the stress during that region, the quasi-static stress, better known as the plateau stress is the highest for the specimen 1. After the quasi-static plateau, the densification region starts and lasts till the strain of 0.38. It can be seen that although the plateau region of the specimens are similar, the densification region varies significantly for each. For the specimen 2 with the pore size of 2.5mm, the densification graph rises gradually with a higher slope until the applied load reaches to 68 kN On the other hand, the specimen 1 undergoes densification till the strain becomes 0.38. It is important to note that after the end of the densification phase, the foams necessarily behave as a solid material under compression. Since the solid compression region does not contribute to impact energy absorption, it is not taken under study.

5. ANALYSIS OF THE RESULTS

When a load is applied on a material, it deforms. The deformation is done by the load against a resisting force, i.e., stress. Therefore, it counts as work done. This work done by the deforming load is stored in the deformed material as strain energy, similar to a spring. This property of a material to absorb the energy as strain energy is called energy absorption. This energy is absorbed from the object that applies the stress on the material, thereby slowing down the material, and making sure that the impact does not transmit to the other side of the material. Since strain energy is nothing but work done on the material, it is directly proportional to both the stress developed in the material and the deformation of the material.

It is also known that in a stress vs strain graph, the area under the graph gives the quantitative value for the energy absorbed through deformation, therefore it can be safely said that the graph which has the largest area under the curve is the best impact absorber. In order to quantitatively determine the energy absorbed, the quasi-static regions of the specimens are neglected because of their small size. The densification region is approximated to a triangle to find the area.

Table 3 Energy Absorption

SPECIMEN NUMBER	STRAIN ENERGY UNIT
Specimen 1	1.726
Specimen 2	2.185

6. CONCLUSION

In the present study, PLA foams of different pore sizes were modelled and 3D printed using Fused Deposition Modeling(FDM) process. The foams were subjected to compression and the stress-strain curves were plotted. Further, simulation studies were conducted on the foams and were compared with experimental results. The dimensional accuracy of the 3D printed porous PLA foams was observed to be accurate. The study revealed that the functionally graded PLA foam have significantly better energy absorbing capacity under low load condition in the linear elastic region and the densification of the cells is more in non-functionally graded foam which contributes greatly to the energy absorption of the foam. The simulation studies exhibited a proximate correlation with experimental results, signifying the validity of the numerical model.

7. REFERENCE

- [1] Paweł Płatek, Kamil Rajkowski, Kamil Cieplak, Marcin Sarzyński, Jerzy Małachowski, Ryszard Woźniak and Jacek Janiszewski Deformation Process of 3D Printed Structures Made from Flexible Material with Different Values of Relative Density.
- [2] Naserddine Ben Ali, Mohamed Khlif, Dorra Gassara Hammami and Chedly Bradai. Mechanical and morphological characterization of spherical cell porous structures manufactured using FDM process
- [3] Whisler D., Kim H. Experimental and simulated high strain dynamic loading of polyurethane foam. Polym. Test.
- [4] Mane J.V., Chandra S. Mechanical Property Evaluation of Polyurethane Foam under Quasi-static and Dynamic Strain Rates—An Experimental Study.
- [5] Linul E., Șerban D.A., Marsavina L., Sadowski T. Assessment of collapse diagrams of rigid polyurethane foams under dynamic loading conditions.
- [6] Ouellet S., Cronin D., Worswick M. Compressive response of polymeric foams under quasi-static, medium and high strain rate conditions
- [7] Castiglioni A., Castellani L., Cuder G., Comba S. Relevant materials parameters in cushioning for EPS foams. Colloids Surf. A Physicochem. Eng.
- [8] Cronin D.S., Ouellet S. Low density polyethylene, expanded polystyrene and expanded polypropylene: Strain rate and size effects on mechanical properties. Polym. Test.
- [9] C. Xia, X.W. Chen, Z. Zhang, (2013), 'Effects of porosity and pore size on the compressive properties of closed-cell Mg alloy foam, Journal of Magnesium and Alloys' Journal of Magnesium and Alloys, Vol. 1, pp.330- 335
- [10] Weeger O, Boddeti N, Yeung S-K, Kaijima S, Dunn M-L. Digital design and nonlinear simulation for additive manufacturing of soft lattice structures
- [11] Ling C, Cernicchi A, Gilchrist M-D, Cardiff P. Mechanical behaviour of

additively-manufactured polymeric octet-truss lattice structures under quasi-static and dynamic compressive loading. Vol. 162, pp.106-118

[12] Gaitanaros S, Kyriakides S. On the effect of relative density on the crushing and energy absorption of open-cell foams under impact. Vol.82, pp.3-13